PHYSICAL REVIEW D VOLUME 22, NUMBER 5 1 SEPTEMBER 1980

Quark diagrams and the Ω^- nonleptonic decays

William A. Ponce
Departamento de Física, Universidad de Antioquia, Medellín, Colombia
(Received 11 March 1980)

The quark-diagram model for nonleptonic two-body baryon decays is discussed and applied to the decay of the Ω^- particle. Current algebra is not employed, but the relation between the quark diagrams and current algebra is explored.

INTRODUCTION

The $\Delta S=1$ effective nonleptonic Hamiltonian calculated originally by Shifman, Vainshtein, and Zakharov (SVZ)[1] in the context of the four-quark model, and by Gilman and Wise[2] in the context of the six-quark model [the Kobayashi-Maskawa[3] (KM) model], has proved to be very useful in the calculation of the S- and P-wave amplitudes for hyperon decays.[4,5] In such calculations the effect of the short-range gluons is taken into account in the Hamiltonian by the use of quantum-chromodynamics (QCD) renormalization effects, and the effect of long-range gluons (confinement effects) is taken into account by the use of the MIT bag[6] wave function for confined quarks.

The effective weak Hamiltonian calculated in Ref. 2 has the form[7]

$$H_{\rm eff}=-\frac{G_F}{\sqrt{2}}\sin\theta_1\cos\theta_1\cos\theta_3 \times(C_1Q_1+C_2Q_2+C_3Q_3+C_5Q_5+C_6Q_6)\,, \quad (1)$$

where θ_i $(i=1,2,3)$ are the three Cabibbo-type angles in the KM model

$$\begin{aligned}
Q_1&=\bar d_i\Gamma_L^\mu s_i\bar u_j\Gamma_{\mu L}u_j+\text{H.c.}\,,\\
Q_2&=\bar d_i\Gamma_L^\mu s_j\bar u_j\Gamma_{\mu L}u_i+\text{H.c.}\\
&=\bar d_i\Gamma_L^\mu u_i\bar u_j\Gamma_{\mu L}s_j+\text{H.c.}\,,\\
Q_3&=\bar d_i\Gamma_L^\mu s_i\bar u_j\Gamma_{\mu L}u_j+\bar d_i\Gamma_L^\mu s_i\bar d_j\Gamma_{\mu L}d_j\\
&\quad+\bar d_i\Gamma_L^\mu s_i\bar s_j\Gamma_{\mu L}s_j+\text{H.c.}\\
&=\bar d_i\Gamma_L^\mu s_i\left(\sum\bar q_j\Gamma_{\mu L}q_j\right)+\text{H.c.}\,, \quad (2)\\
Q_5&=\bar d_i\Gamma_L^\mu s_i\left(\sum\bar q_j\Gamma_{\mu R}q_j\right)+\text{H.c.}\,,\\
Q_6&=\bar d_i\Gamma_L^\mu s_j\left(\sum\bar q_j\Gamma_{\mu R}q_i\right)+\text{H.c.}\\
&=\tfrac{1}{3}Q_5+\tfrac{1}{2}\bar d_i\Gamma_L^\mu\lambda^A s_i\left(\sum\bar q_j\Gamma_{\mu R}\lambda^A q_j\right)\\
&=\tfrac{1}{3}Q_5+\tfrac{1}{2}Q_6'\,,
\end{aligned}$$

where $\Gamma_L^\mu=\gamma^\mu(1+\gamma_5)$, $\Gamma_R^\mu=\gamma^\mu(1-\gamma_5)$, λ^A are color SU(3) matrices normalized by the condition Tr $(\lambda^A\lambda^B)=2\delta^{AB}$, and i and j are color indices. In (2) we have done some Fierz rearrangement in order to make some of the operators better looking, and in order to simplify further calculations. All the Q_i in (2) are normal ordered.

The coefficients C_i in (1) were calculated in Ref. 2 and they are functions of the three Cabibbo-type angles, of the δ phase (the CP-violating phase) of the KM model, of the quark-gluon coupling constant α evaluated at the subtraction point μ, and of some of the masses in the theory (as, for example, m_t, m_b, m_c, M_w, and μ). Some numerical values of C_i are presented in Table I of Ref. 2.

Once the Hamiltonian has been fully determined as in Eqs. (1) and (2), the following task is to calculate the matrix elements of such a Hamiltonian. At the present time, the most satisfactory approach is to use the soft-pion methods of current algebra[8] as is done, for example, in Refs. 4 and 5. The main result from the soft-pion techniques is the parametrization of the amplitude involving a pion in the following way:

$$\langle B'\pi^i|H_{\rm eff}(0)|B\rangle = -\frac{i}{F_\pi}\langle B'|[F_i^5,H_{\rm eff}(0)]|B\rangle+P(q)+R(q)\,, \quad (3)$$

where $F=94$ MeV is the π decay constant and where we denote possible pole terms in (3) as $P(q)$ and absorb into the remainder term $R(q)$ any contribution not included in the first two terms. In a sense, this parametrization tells us nothing since $R(q)$ is unknown. However, we do know that $\lim_{q\to 0}R(q)=0$ and therefore it can be neglected in the first approximation.

In the calculations made in Refs. 4 and 5 for hyperon decays, the commutator term at the right-hand side of (3) gives the main contributions to the parity-violating (PV) S waves and the pole terms $P(q)$ give the main contribution to the parity-conserving (PC) P waves. In Ref. 4 the contribution to $R(q)$ due to the anomalous commutator term was calculated, and in Ref. 5 the equivalent se-

parable contribution to $R(q)$ was determined. The matrix elements of the commutator and of $P(q)$ were evaluated in Refs. 4 and 5 using the MIT bag[6] wave function for hyperons formed from valence quarks in their ground states.

QUARK DIAGRAMS

The soft-pion method for calculating hyperon-decay amplitudes is very useful in order to calculate the first two terms on the right-hand side of Eq. (3), but unfortunately it tells us nothing about the third term $R(q)$. One way to calculate several contributions to $R(q)$ is to use the quark-diagram method.[9] If we neglect final-state weak interactions[10] and assume that the ground-state hyperons are formed only of valence quark, then all the possible quark diagrams that can contribute to nonleptonic baryon decays are exhibited in Fig. 1. Of course, we are working under the approximation that no gluon exchange is occurring between quarks and the only gluon contribution that we are taking into account is the effects of the leading logarithms from QCD that renormalize the weak Hamiltonian.

From the five diagrams in Fig. 1, the easiest one to calculate is 1(e); we calculate it by using

$$\langle Q(q)|A^\mu|0\rangle\langle B'|(V_\mu+A_\mu)|B\rangle = F_Q g_V(B\to B')q^\mu\bar{u}(B')\gamma_\mu(1+\gamma_5)u(B). \quad (4)$$

Notice that in the limit $q\to 0$ this contribution vanishes, so it will contribute to $R(q)$.

If we employ the assumptions which justify the appearance of the short-distance expansion in the derivation of the effective nonleptonic weak Hamiltonian (1), we can cast Fig. 1(d) in the form implied by Fig. 1(e). The W boson is taken to be so massive that its propagator is shrunk to a point. The ensuing four-fermion vertex can be reordered by a Fierz transformation to yield a factorized structure that will give a contribution that is proportional to the contribution given by 1(e). For example, for the particular case when only left-handed currents are considered (Q_1, Q_2Q_3), the color structure of such currents will imply that the contribution from Fig. 1(d) is $\frac{1}{3}$ the contribution from Fig. 1(e).

In the limit $q\to 0$, only Figs. 1(a)–1(c) are nonzero, so in our approximation they are the ones that might contribute to the first two terms on the right-hand side of Eq. (3). As an aside, we note that the resemblance between the baryon pole diagram in Figs. 2(a) and 2(b) and the quark diagrams in Figs. 1(a) and 1(c) is striking; this can be seen, for example, in Fig. 3 where the comparison between Figs. 1(a) and 2(a) is made. As can be seen from the figure, the weak vertex of the baryon pole corresponds to the W exchange in the quark diagram, and the strong vertex corresponds to the creation of a pair by the vacuum in the quark diagram. Similar comparisons can be made between Figs. 1(b) and 1(c) and the pole diagrams in Figs. 2(a) and 2(b).

The graphical analogy that we have indicated in Fig. 3 can also be developed in an analytical way, as is done for example in Ref. 11, where the microscopic equivalent of the baryon poles is derived by the use of Wick's theorems in field theory. Because such an analysis has not been pub-

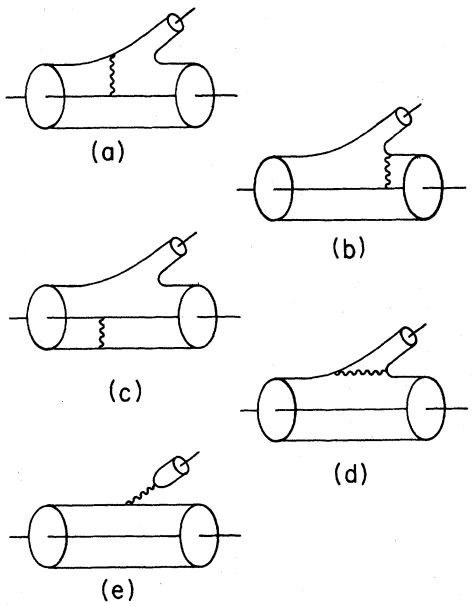

FIG. 1. Quark diagrams that contribute to nonleptonic two-body final-state baryon decays.

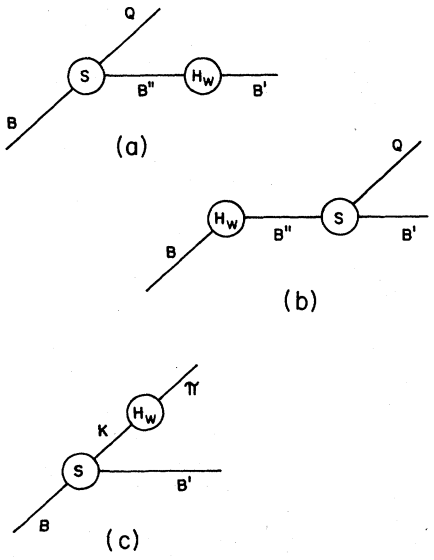

FIG. 2. Pole diagrams.

lished, I will, with the kind permission of the author, reproduce here the highlights of the derivation.

$P(q)$ in Eq. (3) can be written as[8]

$$P(q) = q_\lambda \frac{(m_\pi^2 - q^2)}{F_\pi m_\pi^2} \times \int d^4y\, e^{iq\cdot y} \langle B' | T(A_i^\lambda(y) H_W(0)) | B \rangle , \qquad (5)$$

where the term $P(q)$ will vanish as $q \to 0$ unless there is a pole in the integral at $q = 0$. Let us study the π^- amplitude ($A_{\pi^-}^\lambda = \bar{u}\gamma^\lambda\gamma_5 d$) with the sample Hamiltonian Q_2. Using Wick's theorem to reduce time-ordered products we have

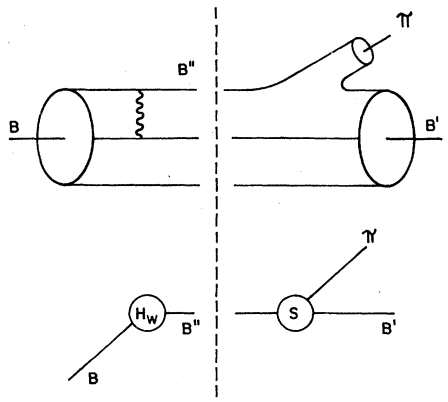

FIG. 3. Graphical relationship between quark and pole diagrams.

$$\begin{aligned} T(A_{\pi^+}^\lambda(y) H_W(0)) &= T(:\bar{u}\gamma^\lambda\gamma_5 d :: \bar{d}\Gamma_L^\mu u u \Gamma_{\mu L} s :) \\ &= :\bar{u}(y)\gamma^\lambda\gamma_5 d(y)\bar{d}(0)\Gamma_L^\mu u(0)\bar{u}(0)\Gamma_{\mu L} s(0): \\ &\quad + :\bar{u}(y)\gamma^\lambda\gamma_5 \langle 0 | T(d(y)\bar{d}(0)) | 0 \rangle \Gamma_L^\mu u(0)\bar{u}(0)\Gamma_{\mu L} s(0): \\ &\quad + :\bar{u}(0)\Gamma_L^\mu s(0)\bar{d}(0)\Gamma_{\mu L} \langle 0 | T(u(0)\bar{u}(y)) | 0 \rangle \gamma^\lambda\gamma_5 d(0): \\ &\quad + \langle 0 | T(:\bar{u}(y)\gamma^\lambda\gamma_5 d(y) :: \bar{d}(0)\gamma_\mu\gamma_5 u(0):) | 0 \rangle \bar{u}(0)\Gamma_L^\mu s(0) , \end{aligned} \qquad (6)$$

where the vacuum expectation values of the time-ordered operators above are the Feynman propagators $S_F(y)$. The second term in the left-hand side of Eq. (6), when sandwiched between baryon states, describes the weak Hamiltonian acting at $x = 0$, the baryon propagating as a three state to $x = y$, where one of the quarks interacts with the axial current. The diagrammatic picture of the first three terms is given in Figs. 4(a)–4(c), respectively. They are the microscopic equivalent of the baryon poles and they very much resemble the quark diagrams in Figs. 1(a)–1(c). The fourth term is represented in Fig. 4(d).

To handle the fourth term, the PCAC (partial conservation of axial-vector current) relation and the Lehmann-Symanzik-Zimmermann reduction can be used in reverse to prove that it is equivalent to

$$\langle \pi^+ | \bar{d}\gamma_\mu\gamma_5 u | 0 \rangle \langle B' | \bar{u}\Gamma_L^\mu s | B \rangle ,$$

i.e., the fourth term is related to Figs. 1(d) and 1(e) and it belongs therefore to $R(q)$ in Eq. (3) and not to $P(q)$. Because of the former arguments we are going to assume from now on that the quark diagrams in Figs. 1(a)–1(c) are related to pole diagrams, and will give contributions to $P(q)$ in Eq. (3) and the diagrams in Figs. 1(d) and 1(e) will give contributions to $R(q)$ in (3). Finally, notice that Fig. 1(d) can be related to the K pole diagram in Fig. 2(c). Therefore, our conclusion is that the quark-diagram method as described here can give us information about the pole terms and the remainder terms in Eq. (3), but not about the commutator term.

Next, we will apply this model to the decay of the Ω^- particle.[12,13]

As can be seen, our analysis will coincide with the analysis made in Ref. 12 for the pole terms

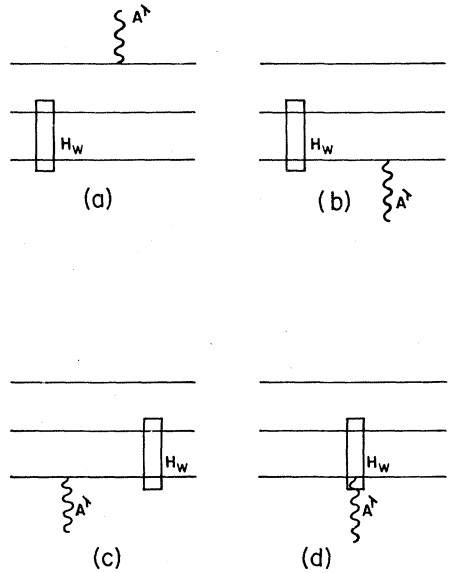

FIG. 4. Microscopic equivalent of the baryon poles.

and it will improve our understanding of the analysis made for $R(q)$ in the same reference.

NONLEPTONIC DECAYS OF Ω^-

In general there is only phase space available for the following $\Delta S=1$ nonleptonic weak decays of Ω^- into two-body final states:

$$\Omega^- \to \Xi^0\pi^-\,,\quad \Omega^- \to \Xi^-\pi^0\,,\quad \Omega^- \to \Xi^{0*}\pi^-$$
$$\Omega^- \to \Lambda^0 K^-\,,\quad \Omega^- \to \Xi^{-*}\pi^0\,.$$

From those we will consider only the first three decays, where a spin-$\frac{3}{2}$ particle (a Rarita-Schwinger field) decays into a spin-$\frac{1}{2}$ particle and a pseudoscalar meson. The invariant amplitude M for those decays $[\Omega(p)\to B(p')+\varphi(K)]$ can be written as

$$M=\frac{K^\lambda}{m_\Omega}\,\bar{u}(p')(B+\gamma_5 A)U_\lambda(p)\,, \tag{7}$$

where U_λ is the Rarita-Schwinger vector spinor field, u is a Dirac field, B is the PC amplitude, and A is the PV amplitude.

From (7) the decay probability is

$$\Gamma=\frac{|\vec{P}|^3[|B|^2(P_0'+m')+|A|^2(P_0'-m')]}{12\pi m_\Omega{}^3}\,, \tag{8}$$

where

$$P_0'=\frac{m_\Omega{}^2+m'^2-m_\varphi{}^2}{2m_\Omega}\quad\text{and}\quad |\vec{P}|^2=P_0'^2-m'^2\,.$$

As we can see from (8), the PV amplitude $|A|^2$ is suppressed by a phase-space factor of the order of 10^{-2} compared with the PC amplitude $|B|^2$. For that reason we will concentrate on the calculation of $|B|^2$, under the assumption that both amplitudes are of the same order of magnitude.

According to Eq. (3), B is given by

$$B=\langle B(p')\varphi_i(K)|H_{\rm eff}(\mathrm{PC})|\Omega^-(p)\rangle$$
$$=-\frac{i}{F_\pi}\langle B'|[F_i^5,H_{\rm eff}(\mathrm{PC})]|\Omega^-\rangle+P(q)+R(q)\,,$$

where the commutator term is given by[4]

$$\langle B'|[F_i^5,H_{\rm eff}(\mathrm{PC})]|\Omega^-\rangle$$
$$=-\tfrac{1}{2}\langle B'|H_{\rm eff}(\mathrm{PV})|B\rangle+\langle\theta^0\rangle\,. \tag{9}$$

The first term in (9) is zero due to the SU(3) of flavor symmetry[14] (a calculation of this term using the MIT bag wave functions will also give zero due to the orthogonality of the spin integrals). The anomalous commutator term[4] $\langle\theta^0\rangle$ can be calculated here and neglected in the calculation of $R(q)$, or it can be calculated as a contribution to $R(q)$ and be neglected here (double counting must be avoided). We are going to use the latter approach, neglecting the commutator term entirely here. Then the amplitude B will have contributions only from quark diagrams as in Fig. 1. In order to draw such diagrams seven pieces of the Hamiltonian must be considered; they are

$$\begin{aligned}
H_1(LL)&=Q_2\,,\\
H_2(LL)&=Q_1\,,\\
H_2(LR)&=\bar{d}_i\,\Gamma_L^\mu\, s_i\,\bar{u}_j\,\Gamma_{\mu R}\,u_j\,,\\
H_3(LL)&=\bar{d}_i\,\Gamma_L^\mu\, s_i\,\bar{d}_j\,\Gamma_{\mu L}\,d_j\,,\\
H_3(LR)&=\bar{d}_i\,\Gamma_L^\mu\, s_i\,\bar{d}_j\,\Gamma_{\mu R}\,d_j\,,\\
H_4(LL)&=\bar{d}_i\,\Gamma_L^\mu\,\bar{s}_i\,\bar{s}_j\,\Gamma_{\mu L}\,\bar{s}_j\,,\\
H_4(LR)&=\bar{d}_i\,\Gamma_L^\mu\,\bar{s}_i\,\bar{s}_j\,\Gamma_{\mu R}\,\bar{s}_j\,.
\end{aligned} \tag{10}$$

The operator Q_6' involving λ^4 matrices does not need to be included here due to the relationships $\langle Q_6'\rangle=\frac{16}{3}\langle Q_5\rangle$ for factorization diagrams,[1] and $\langle Q_6'\rangle=-\frac{8}{3}\langle Q_5\rangle$ for pole diagrams.[4]

Now in order to evaluate the invariant amplitude, all the possible quark diagrams must be drawn between the initial and the final state under consideration. Then we must evaluate such diagrams for the PC Hamiltonian only. In Fig. 5 we have the three possible quark diagrams for the decay $\Omega'\to\pi^-\Xi^0$. The values of those diagrams together with the results for the other decays is presented in Table I, where the notation[15] is

$$\begin{aligned}
g&=g_{\Omega^-\Xi^0K^-}=13.5\,,\\
I&=\langle\pi^-|A^\mu|0\rangle\langle\Xi^0|A_\mu|\Omega^-\rangle\,,\\
I_A&=\frac{N_u{}^3N_s}{(4\pi)^2}\int d^3x\left(j_0(\delta_u)j_0(\delta_s)-\frac{j_1(\delta_u)j_1(\delta_s)}{(\epsilon_u\epsilon_s)^{1/2}}\right)\\
&\qquad\times(u\to u,s\to u)\,,\\
I_B&=\frac{N_u{}^3N_s}{(4\pi)^2}\int d^3x\left(\frac{j_0(\delta_u)j_1(\delta_s)}{\sqrt{\epsilon_s}}+\frac{j_1(\delta_u)j_0(\delta_s)}{\sqrt{\epsilon_u}}\right)\\
&\qquad\times(u\to u,s\to u)\,,\\
\delta_i{}^2&=(\omega_i{}^2-m_i{}^2R)\,,\\
\epsilon_i&=\frac{\omega_i+m_iR}{\omega_i-m_iR}\,,\\
N_i{}^2&=\frac{\delta_i{}^4}{R^3(2\omega_i{}^2-2\omega_i+m_iR)\sin^2\delta_i}\,.
\end{aligned} \tag{11}$$

I_A^* and I_B^* are the same as I_A and I_B, with the replacement $u\to s$. R is the bag radius, j_0 and j_1 are spherical Bessel functions, and ω is the frequency for the quark inside the bag.

The entries in Table I with the integrals I_B, I_B, I_A^*, I_B^* belong to pole diagrams and were evaluated using the MIT bag wave function, while the strong coupling constants were determined by using the SU(3) of flavor symmetry. The entries

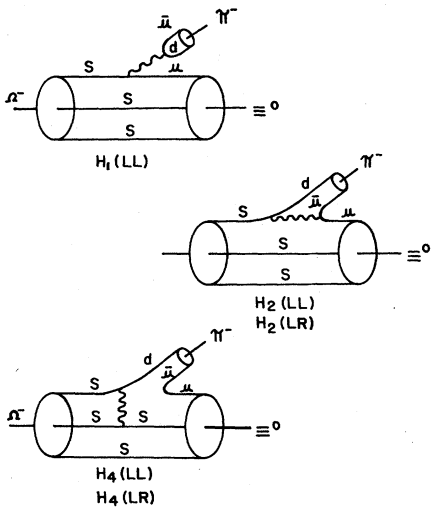

FIG. 5. Quark diagrams for the decay $\Omega^- \to \Xi^0\pi^-$.

with the parameter I belong to factorization diagrams. Quark masses in Table I refer to current quark masses that are different from constituent quark masses in Eq. (11).

If we use the entries in Table I with the SVZ Hamiltonian[1] we get results consistent with those in Ref. 12. Instead, we will use the Hamiltonian in Ref. 2, and also the following parameters:

$$\langle \pi^- | A^\mu | 0 \rangle \langle \Xi^0 | A_\mu | \Omega^- \rangle = \frac{\epsilon F_\pi^{\,2}}{m_\pi},$$

where $\epsilon = 2.15$ is a parameter that measures the form factor $\langle \Xi^- | \partial_\mu A^\mu | \Omega^- \rangle = \epsilon F_\pi / m_\pi$. The constituent quark masses we use in order to evaluate the bag integrals are $m_u = m_d = 0$ and $m_s = 340$ MeV. The current quark masses we use are $m_u = 5$ MeV, $m_d = 7.5$ MeV, and $m_s = 150$ MeV; the renormalization parameter Z takes the value[4] 0.48. The Cabibbo-type angles are such that $\cos\theta_3 \approx 1$, and $\sin\theta_1 = 0.23$. For those numbers the bag integrals are

$$I_A = 0.95 \times 10^{-3}, \quad I_B = 1.15 \times 10^{-3},$$
$$3I_A^* + I_B^* = 3.26 \times 10^{-3}.$$

Our final numerical results are presented in Table II. The entries in the table should be compared with the following experimental results[16]:

$$|B(\Xi^0\pi^-)| = 22.19 \times 10^{-7},$$
$$|B(\Xi^-\pi^0)| = 13.18 \times 10^{-7},$$
$$|B(\Lambda^0 K^-)| = 67.70 \times 10^{-7}.$$

The six entries for B in Table II are for the six sets of parameters presented in Table I of Ref. 2. As we can see the agreement with the experimental results is close for several sets of the parameters.

CONCLUSIONS

By assuming that the quark diagrams in Fig. 1 can contribute only to the noncommutator terms in Eq. (3), and that Figs. 1(a)–1(c) correspond to pole diagrams, we have obtained a very consistent scheme which is successful in evaluating nonleptonic decays for Ω^-.

It is our position that the restrictions we have imposed in the model, especially the one that identifies Figs. 1(a)–1(c) with pole diagrams, are due to our lack of mathematical tools in order to evaluate more precisely the quark diagrams. It could be that the quark diagrams also give information about the commutator term, but then a more sophisticated technique must be developed to evaluate them before reaching final conclusions.

The most pleasing aspect of our calculations is the way we handle the factorization diagrams, especially for $H_i(LR)$. As can be seen from Table I, not all the entries under the columns $H_i(LR)$ are enhanced by the mass ratios, only the ones associated with Fig. 1(d) are so enhanced. Another point is that such enhancement is different for $H_2(LR)$ than for $H_3(LR)$, due to the fact that different quark masses are present.

The calculations in this paper are similar to the ones presented in Ref. 12. Not only are the quark dynamics the same in both papers but our Table I (with a few changes) can reproduce the numbers in Ref. 12. If this is the case, then why are our

TABLE I. Structure of the quark diagrams for the Ω^- decay. The factors are defined in Eq. (11).

Decay	$H_1(LL)$	$H_2(LL)$	$H_2(LR)$	$H_3(LL)$	$H_3(LR)$	$H_4(LL)$	$H_4(LR)$
$(\Xi^0\pi^-)$	I	$I/3$	$\frac{-2m_\pi^{\,2}IZ^2}{3(m_u+m_d)(m_u+m_s)}$	0	0	0	$\frac{4g(3I_A^*+I_B^*)}{3(m_\Omega - m_{\Xi^*})}$
$\sqrt{2}(\Xi^-\pi^0)$	$I/3$	I	$-I$	$-4I/3$	$I+\frac{m_\pi^{\,2}IZ^2}{3m_d(m_d+m_s)}$	0	$\frac{4g(3I_A^*+I_B^*)}{3(m_\Omega - m_{\Xi^*})}$
$(\Lambda^0 K^-)/\sqrt{6}$	$\frac{-2g(I_A+I_B)}{(m_\Xi - m_\Lambda)}$	$\frac{2g(I_A+I_B)}{(m_\Xi - m_\Lambda)}$	$\frac{-g(I_A-I_B)}{(m_\Xi - m_\Lambda)}$	0	0	0	$\frac{2g(3I_A^*+I_B^*)}{3(m_\Omega - m_{\Xi^*})}$

TABLE II. Numerical study of the decay amplitude $|B|$ for Ω^- decays. All the entries are in units of 10^{-7}. The values for C_i are taken from Table I in Ref. 2.

Decay	Mode	$\alpha=0.75$ $m_t=15$ GeV	$\alpha=1.00$ $m_t=15$ GeV	$\alpha=1.25$ $m_t=15$ GeV	$\alpha=0.75$ $m_t=30$ GeV	$\alpha=1.00$ $m_t=30$ GeV	$\alpha=1.25$ $m_t=30$ GeV
$(\Xi^0\pi^-)$	Factorization	10.44	11.68	12.90	10.38	11.10	12.82
	Pole	0.24	0.43	0.62	0.24	0.43	0.61
$(\Xi^-\pi^0)$	Factorization	1.96	3.06	3.80	1.92	2.84	3.75
	Pole	0.17	0.30	0.44	0.17	0.30	0.43
$(\Lambda^0 K^-)$	Factorization	0.0	0.0	0.0	0.0	0.0	0.0
	Pole	25.59	28.59	31.22	25.34	28.35	30.98

final numbers not as close to the experimental results as the ones obtained in Ref. 12? First, by using the more realistic set of coefficients C_i in Ref. 2 rather than those in Ref. 1, we find that the contributions coming from the left-right operators Q_5 and Q_6 are not as large as we would like them to be. In Ref. 2 not only is the calculation done in the six-quark model, but the substraction point u is not required to be as small as in Ref. 1. Second, by using the renormalized quark masses instead of the unrenormalized ones,[4] we pick up an extra factor of Z^2 in the enhancement coefficient for $H_i(LR)$. This will lower the contributions from those terms by about a factor of 4. Finally, some of our bag integrals are a little smaller than the ones calculated in Ref. 12. Because of the first and the last reasons above, our pole contributions are smaller by about a factor of 10, and because of the first two, our factorization contributions for Q_5 and Q_6 are appreciably smaller. Therefore, our conclusions here are similar to those presented in Ref. 4: The inclusion of the left-right operators tends to improve the results, but the values of the enhancement coefficients C_5 and C_6 have to be larger (by about a factor of 10) in order to have a good agreement with the experimental results. Here, as in Ref. 4, it may well be the case that the pole model, at least in its present form, is unable to adequately represent the experimental situation.

We hope that the analysis presented here serves to provide a deeper insight in the evaluation of the so-called factorization diagrams, and to improve our overall understanding of the evaluation of matrix elements.

ACKNOWLEDGMENTS

I would like to thank E. Golowich for useful conversations concerning the subject presented here. Part of this work was done at the University of Massachusetts at Amherst.

[1]M. A. Shifman, A. I. Vainshtein, and V. J. Zakharov, Nucl. Phys. B120, 315 (1977); Report Nos. ITEP-63 and ITEP-64 (unpublished).

[2]F. J. Gilman and M. B. Wise, Phys. Rev. D 20, 2392 (1979).

[3]M. Kobayashi and K. Maskawa, Prog. Theor. Phys. 49, 652 (1973).

[4]J. F. Donoghue, E. Golowich, W. A. Ponce, and B. R. Holstein, Phys. Rev. D 21, 186 (1980).

[5]H. Galić, D. Tadić, and J. Trampetić, Nucl. Phys. B158, 306 (1979).

[6]A. Chodos, R. L. Jaffe, K. Johnson, C. B. Thorn, and V. F. Weisskopf, Phys. Rev. D 9, 3471 (1974); A. Chodos, R. L. Jaffe, K. Johnson, and C. B. Thorn, *ibid.* 10, 2599 (1974).

[7]In Ref. 2, H_{eff} is calculated under the assumption that the vertex induced by the penguin diagram is a local one.

[8]See, for example, R. E. Marshak, Riazuddin, and C. R. Ryan, *Theory of Weak Interactions in Particle Physics* (Wiley-Interscience, New York, 1964).

[9]The way we use the quark diagrams here is the same one proposed by J. F. Donoghue and E. Golowich, Phys. Rev. D 14, 1386 (1976).

[10]If final-state weak interactions are considered, two more diagrams must be added in Fig. 1.

[11]J. F. Donoghue, doctoral dissertation, University of Massachusetts, 1976 (unpublished).

[12]H. Galić, D. Tadić, and J. Trampetić, Phys. Lett. 89B, 249 (1980).

[13]Calculations previous to Ref. 12 to Ω^- nonleptonic decays are in J. Finjord, Phys. Lett. 76B, 116 (1978); L. R. R. Mohan, Phys. Rev. D 1, 266 (1970); Y. Hara, Phys. Rev. 150, 1175 (1966).

[14]B. W. Lee and A. R. Swift, Phys. Rev. 136, B228 (1964).

[15]The following SU(3)-of-flavor relations were used in Table I:

$$g = g_{\Omega^-\Xi^0K^-} = \sqrt{2}\, g_{\Xi^*\Lambda^0K^-} = \sqrt{3}\, g_{\Xi^*\Xi^0\pi^-} = \sqrt{6}\, g_{\Xi^*\Xi^-\pi^0}.$$

[16]M. Bourquin *et al.*, Phys. Lett. 88B, 192 (1979).